

# Real-Time Per-Garment Virtual Try-On with Temporal Consistency for Loose-Fitting Garments

Zaiqiang Wu  
The University of Tokyo  
Japan

I-Chao Shen  
The University of Tokyo  
Japan

Takeo Igarashi  
The University of Tokyo  
Japan



(a) Real-time virtual try-on



(b) Loose-fitting garment try-on results

**Figure 1.** (a) Our virtual try-on system features an efficient inference pipeline that enables real-time performance. (b) Our method produces highly realistic 360° virtual try-on results for loose-fitting garments with temporal consistency.

## Abstract

Per-garment virtual try-on methods collect garment-specific datasets and train networks tailored to each garment to achieve superior results. However, these approaches often struggle with loose-fitting garments due to two key limitations: (1) They rely on human body semantic maps to align garments with the body, but these maps become unreliable when body contours are obscured by loose-fitting garments, resulting in degraded outcomes; (2) They train garment synthesis networks on a per-frame basis without utilizing temporal information, leading to noticeable jittering artifacts. To address these challenges, we propose a two-stage approach for robust semantic map estimation. First, we extract a garment-invariant representation from the raw input image. This representation is then passed through an auxiliary network to estimate the semantic map. This enhances the robustness of semantic map estimation under loose-fitting garments during garment-specific dataset generation. Furthermore, we introduce a recurrent garment synthesis framework that incorporates temporal dependencies to improve frame-to-frame coherence while maintaining real-time performance. We conducted qualitative and quantitative evaluations to demonstrate that our method outperforms existing approaches in both image quality and temporal coherence. Ablation studies further validate the

effectiveness of the garment-invariant representation and the recurrent synthesis framework.

**CCS Concepts:** • Computing methodologies → Image processing; Image-based rendering; • Human-centered computing → Mixed / augmented reality.

**Keywords:** Virtual Try-On, Image Synthesis, Human-in-the-loop Machine Learning

## 1 Introduction

Virtual try-on technology enables customers to try on garments without physical access, has recently garnered significant attention from researchers in today’s e-commerce landscape. Existing image-based virtual try-on methods [7, 10, 12, 22, 25, 30] require only a 2D in-shop image of the target garment to generate virtual try-on results, making them highly accessible. However, these approaches are predominantly tailored for retailers aiming to produce promotional images featuring fashion models, rather than for end-users seeking personalized virtual try-on experiences. This focus is clearly reflected in the biased datasets used for training, which are heavily skewed toward tall and slim fashion models. As a result, these methods fail to generalize well to the diverse body types of average consumers.

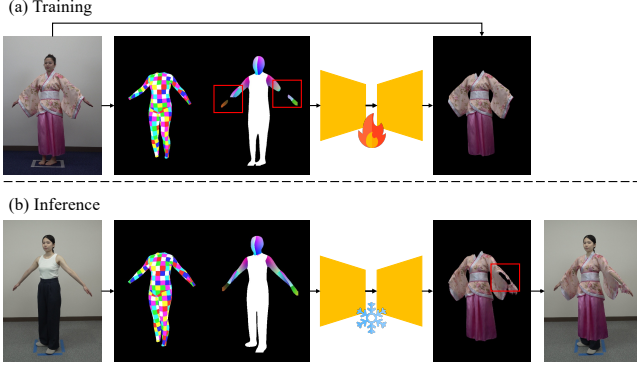


**Figure 2.** Illustration of the training and inference pipelines for applying the method proposed in [54] to virtually try on a loose-fitting garment. (a) During training, the garment synthesis network is trained using degraded DensePose [17] outputs. (b) During inference, a distribution mismatch between training and input data leads to suboptimal garment synthesis results.

Unlike general image-based methods, per-garment virtual try-on methods [8, 54, 55] focus on customer-oriented virtual try-on by collecting garment-specific datasets and training garment-specific neural networks. Early per-garment methods [8, 55] require an expensive robotic mannequin for dataset collection, making their results non-reproducible. [54] lower the barrier to dataset collection significantly by using real human bodies for dataset collection. This approach relies on DensePose [17] for estimating human body semantic maps, which are crucial for aligning the human body and the synthesized garment in 2D image space. However, it struggles with *loose-fitting* garments, as DensePose results degrade significantly for these types of clothing, causing a distribution discrepancy between the training and inference stages, as illustrated in Figure 2. Such discrepancies lead to degraded results during the inference stage, where users typically wear tight-fitting garments to facilitate accurate human body tracking.

Moreover, previous per-garment approaches rely solely on the current input frame for garment synthesis, neglecting the *temporal continuity* provided by preceding frames. As a result, their results often exhibit jittering artifacts—especially for loose-fitting garments, which naturally exhibit appearance variations even under identical poses.

To address these limitations, we introduce a garment-invariant representation that can be directly extracted from the raw input image. This representation is then transformed into a human body semantic map using an auxiliary network, enabling robust estimation of the human body semantic map under loose-fitting garments during garment-specific dataset generation. The garment-invariant representation leverages joint heatmaps and 3D human pose, both of which are inherently robust to garment variations. Furthermore, we propose

a recurrent garment synthesis framework that ensures temporal consistency by conditioning the synthesis process on both the current input frame and the preceding temporal states.

Our recurrent garment synthesis framework is capable of processing input sequences of arbitrary length while maintaining high efficiency, achieving approximately 10 frames per second on a standard PC. This ensures a smooth and responsive virtual try-on experience for users, as demonstrated in Figure 1. Both qualitative and quantitative evaluations indicate that our method surpasses existing approaches in terms of visual quality and temporal consistency. We also conduct ablation studies to validate the necessity of the garment-invariant representation and the recurrent synthesis framework.

Our contributions can be summarized as follows:

- We propose a garment-invariant representation for robust human body semantic map estimation under loose-fitting garments, enabling per-garment virtual try-on for such garments.
- We develop a recurrent garment synthesis framework that supports real-time virtual try-on with temporal consistency, accommodating input sequences of arbitrary length.
- We conduct comprehensive qualitative and quantitative comparisons with existing methods, along with ablation studies, to validate the effectiveness and necessity of each component in our proposed framework.

## 2 Related Work

### 2.1 3D model-based Virtual Try-On

3D model-based virtual try-on methods [16, 36, 37, 41, 44] typically represent garments using polygon meshes. These methods generate try-on results by simulating the interaction between clothing and a 3D human body model, leveraging either physics-based simulations [9, 24, 35, 45] or learning-based approaches [3, 15, 18, 29, 36, 37, 41–43, 56]. While these techniques can realistically capture garment deformations across diverse poses and viewpoints, they require labor-intensive manual 3D modeling for each garment, which poses a significant barrier to scalability. To address this, some recent approaches [1, 5, 6, 11, 14, 19, 31, 32] adopt volumetric representations, such as Neural Radiance Fields (NeRF) [34] and 3D Gaussian Splatting (3DGS) [26], to model garments directly from monocular images. These representations facilitate automatic 3D garment reconstruction but are primarily designed for digital avatars and are not optimized for real-time virtual try-on experiences involving real human users.

In contrast, our method supports real-time virtual try-ons for real-world users and enables automatic pre-processing for each garment with minimal human intervention.

## 2.2 Image-based Virtual Try-On

Image-based virtual try-on methods eliminate the need for 3D modeling of garments, relying instead on a single 2D in-shop image to generate try-on results [47]. This makes them significantly more accessible and scalable compared to 3D model-based approaches. Several methods [7, 22, 28, 30, 52, 57] focus on producing static try-on images, which lack the ability to convey dynamic garment behavior. To address this, other approaches [4, 10, 12, 23, 25, 58] incorporate inter-frame consistency to generate temporally coherent video try-on results. However, these methods typically suffer from high memory usage, restricting the length of video they can process. It is also important to note that most existing image-based virtual try-on systems are designed primarily for e-commerce retailers to showcase garments on idealized fashion models for marketing purposes. Their networks are typically trained on datasets biased toward tall and slim body types, resulting in suboptimal performance when applied to average users.

In contrast, our method is designed for customer-centric virtual try-ons and supports real-time virtual try-on with temporal consistency for arbitrary lengths of input frames.

## 2.3 Per-garment Virtual Try-On

Unlike image-based virtual try-on approaches that rely on universal networks trained across diverse garment types, per-garment methods focus on training garment-specific networks using dedicated datasets, resulting in superior try-on quality for specific garments. A pioneering effort by [8] introduced the use of a robotic mannequin to automate the collection of garment-specific datasets, enabling the training of garment-specific networks. However, this approach requires users to wear a physical measurement garment for accurate body tracking, which limits its practicality. To address this, [55] proposed a vision-based intermediate representation that eliminates the need for the physical measurement garment. More recently, [54] further reduced the barrier to dataset collection by leveraging real human bodies, thereby removing the dependency on costly robotic mannequins. Despite these advancements, [54] struggles with loose-fitting garments due to their reliance on human body semantic map estimation, which often fails under such garments, and the jittering artifacts resulting from a lack of inter-frame consistency enforcement.

Our method addresses these limitations by introducing a garment-invariant representation for human body semantic map estimation and a recurrent garment synthesis framework, enabling high-quality dataset generation and temporally consistent virtual try-ons for loose-fitting garments.

## 2.4 Domain Adaption

Domain adaptation aims to ensure the performance of machine learning models trained on a source domain when applied to a target domain with a different data distribution [13]. The predominant paradigm of domain adaptation is mapping the source and target domains into a shared space [20, 40, 49–51]. [20] present a domain adaptation framework with fully convolutional networks for semantic segmentation. They learn the mapping to the shared space in an unsupervised manner by assuming source and target domains share the same label statistics. [21] directly learns the mapping from the source domain to the target domain in a supervised way. However, the correlations between the source and target domain are usually unknown. [39] and [59] use cycle consistency to learn the mappings between unpaired source and target images. However, unpaired image-to-image translation struggles with high-resolution images, limiting their applicability in our scenario.

In this paper, we propose a shared representation space for images of humans wearing tight-fitting and loose-fitting garments. Our aim is to bridge the domain gap that causes existing human body semantic map estimation models, trained predominantly on tight-fitting garment images, to underperform when applied to loose-fitting garment images.

# 3 Method

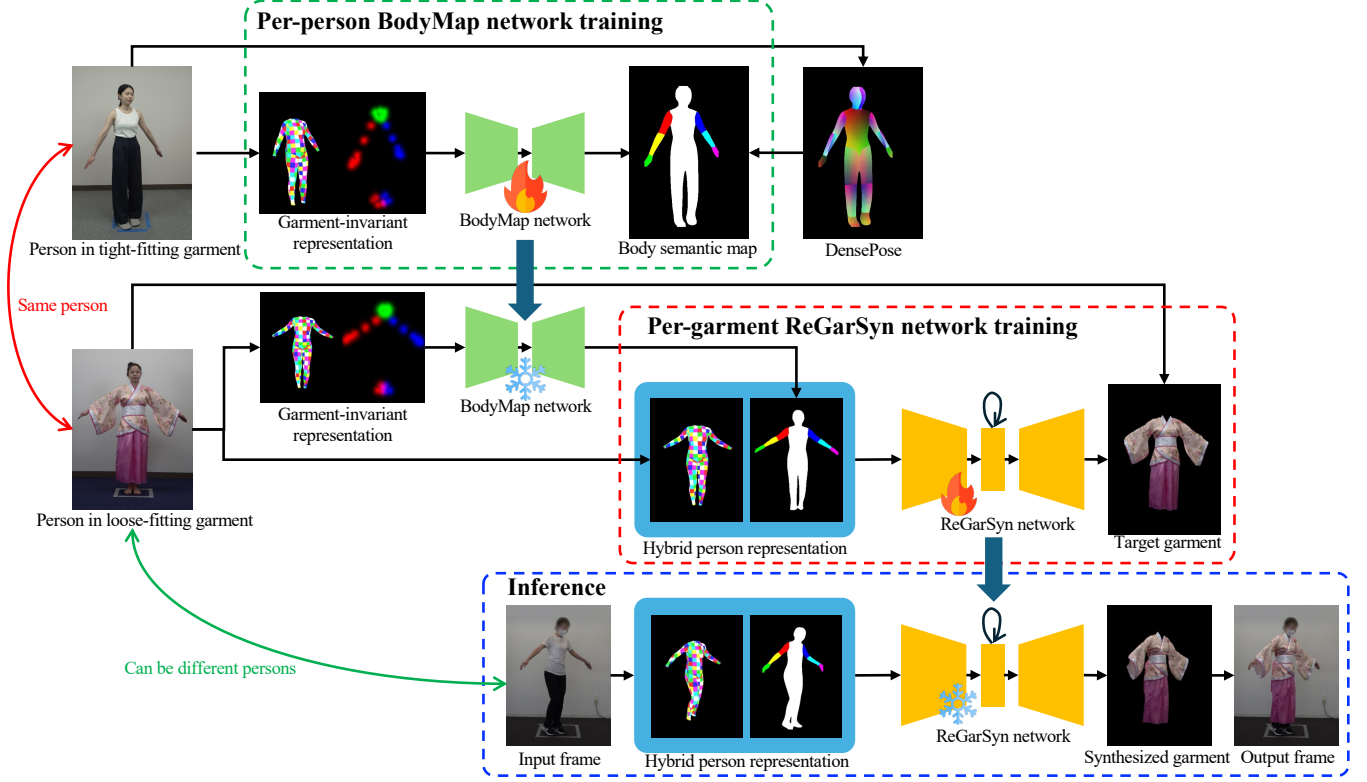
## 3.1 Overview

Figure 3 provides an overview of our method. To mitigate the distribution gap between the training and inference stages, we aim to obtain robust human body semantic maps under loose-fitting garments. To achieve this, we first train a per-person BodyMap network using images of a person wearing arbitrary tight-fitting garments. This network can then be used to robustly estimate body semantic maps for the same person in the target loose-fitting garment by transforming the extracted garment-invariant representations into body semantic maps.

Subsequently, these estimated maps are used to train a per-garment Recurrent Garment Synthesis (ReGarSyn) network that learns the mapping from the input sequence to the target garment image sequence. Once trained, the ReGarSyn network enables real-time, temporally consistent virtual try-ons for arbitrary persons.

## 3.2 Design of Garment-Invariant Representation

[54] employ DensePose [17] for estimating the human body semantic map directly from the raw input image. However, DensePose varies significantly under loose-fitting garments, as shown in Figure 4. To ensure reliable human body semantic map estimation under loose-fitting garments, we need a garment-invariant representation that captures human body information and is invariant to the garment to serve as the intermediate representation. A natural candidate for such a



**Figure 3.** Overview of our method. We first train a per-person BodyMap network using images of a person wearing tight-fitting garments. This network is then used to robustly estimate body semantic maps for the same person in a loose-fitting garment. These estimated maps are subsequently used to train a per-garment ReGarSyn network. Once trained, the ReGarSyn network enables real-time virtual try-on for arbitrary persons.



**Figure 4.** DensePose [17] accurately estimates the human body semantic map when subjects wear tight-fitting garments (left). However, its performance significantly degrades with loose-fitting garments due to occlusions (right).

representation is the set of human joints. However, not all joints are truly garment-invariant. The presence and type of garments can influence their detected positions and associated confidence scores, as shown in Figure 12. The human joint estimation results are generated by Sapiens [27], which is the state-of-the-art human pose estimation method.

Although human joint estimation is not entirely garment-invariant, it can still serve as a robust representation by excluding joints sensitive to garment variations, such as the hips and knees. However, excluding these joints limits

the expressiveness of the resulting pose representation. To address this limitation, we augment the remaining joint data with virtual measurement garment [54], which is a rendered image of the SMPL mesh that encapsulates the full 3D human pose. In contrast to [54], which uses an upper-body template mesh, we utilize a full-body template mesh to facilitate the representation of full-body pose.

As illustrated in Figure 5, given an input person image  $I \in \mathbb{R}^{3 \times H \times W}$ , we first estimate the 3D human pose using BEV [48], which outputs a SMPL mesh [33]. To ensure garment invariance, we fix the body shape parameters that are sensitive to garment variations. Subsequently, we remove non-essential body parts (head, hands, and feet) and apply a grid-pattern texture to the remaining mesh. This textured mesh is then rendered into an RGB image  $I_{vm} \in \mathbb{R}^{3 \times H \times W}$ .

In parallel, we extract 133 joint heatmaps using Sapiens [27]. To further reduce sensitivity to garment variation, we discard the heatmaps corresponding to the hip and knee joints. The remaining heatmaps are grouped into three categories and compactly represented as an RGB image  $I_{shm} \in \mathbb{R}^{3 \times H \times W}$ .

Combining these components, we construct our proposed garment-invariant representation  $I_{gi} \in \mathbb{R}^{6 \times H \times W}$  as follows:



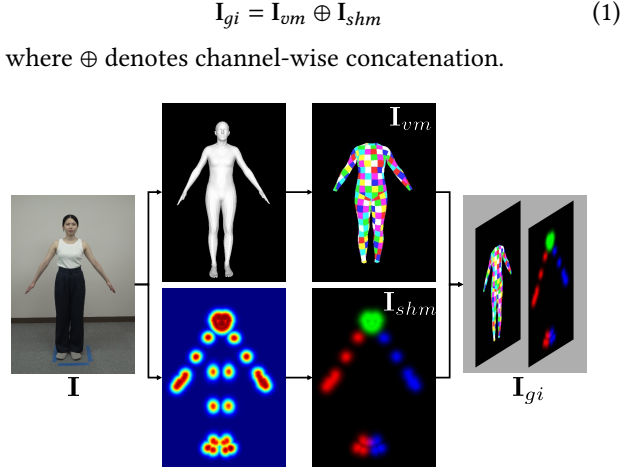


**Figure 5.** Garment-invariant representation extraction from a person image.

### 3.3 Reliable Human Body Semantic Map Estimation

Unlike [54], which employs a simplified DensePose map as the human body semantic representation, our approach utilizes an even more simplified version, in which continuous UV coordinates are removed, as illustrated in Figure 6. This quantization enhances the learnability of the mapping from a garment-invariant representation to the human body semantic map. Following [54], we merged the lower and upper torso regions in the DensePose map. This was motivated by the observation that the boundary between these regions is not invariant to garment type, even for tight-fitting garments, as demonstrated in Figure 11.

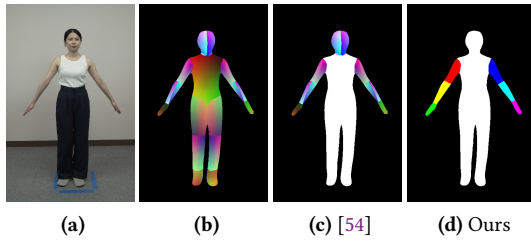


**Figure 6.** Visual illustration of human body semantic maps: (a) The input image; (b) The DensePose map; (c) The human body semantic map of [54]; (d) The human body semantic map of ours.

We obtain the human body semantic map through a two-step process: First, we extract the garment-invariant representation from the input image. Next, we transform this garment-invariant representation into the human body semantic map using a per-person BodyMap network.

To generate the training data for the BodyMap network tailored to a specific person, we record a video of the person wearing a tight-fitting garment while performing predefined movements, as described in [54]. This person will later serve as the human model for per-garment dataset collection.

As illustrated in Figure 3, we use the recorded video to generate paired garment-invariant representations and human body semantic maps to train a BodyMap network, whose architecture follows pix2pixHD [53]. The BodyMap network is then used to estimate the human body semantic map of the same person wearing a loose-fitting garment.

The BodyMap network is trained on a per-person basis and does not generalize across individuals. While this necessitates collecting a dedicated dataset for each human model, the process remains accessible, as it does not rely on specialized sensors to capture the body’s semantic map beneath loose-fitting garments. Moreover, since we typically use the same human model to collect multiple per-garment datasets, the trained BodyMap network can be efficiently reused.

### 3.4 Dataset Generation for Loose-Fitting Garments

For each garment item, we collect a garment-specific dataset, hereafter referred to as a per-garment dataset, to enable the training of garment-specific networks. Similar to the procedure in [54], we record a video of the human model wearing the loose-fitting garment performing predefined movements. In addition, we record a video of the same human model wearing an arbitrary tight-fitting garment and performing the same predefined movements, which is used to train the BodyMap network.

As illustrated in Figure 7, given a frame  $\mathbf{I}$  of the loose-fitting garment videos, we obtain the garment image  $\mathbf{I}_g$  and garment mask  $\mathbf{I}_m$  using SAM2 [38]. Then, we obtain the virtual measurement garment image  $\mathbf{I}_{vm}$ , which is also used to construct the garment-invariant representation  $\mathbf{I}_{gi}$ . By inputting the garment-invariant representation into the trained BodyMap network, we obtain the human body semantic map  $\mathbf{I}_{sdp}$  robustly under loose-fitting garments.

After processing each frame of the loose-fitting garment video to obtain its corresponding  $\mathbf{I}_g$ ,  $\mathbf{I}_m$ ,  $\mathbf{I}_{vm}$ , and  $\mathbf{I}_{sdp}$ , we finish generating the per-garment dataset for the loose-fitting garment. We preserve the sequential order of each frame in the dataset to utilize temporal information for training.

### 3.5 Training Pipeline of Virtual Try-On

We follow [54] to utilize hybrid person representation as the intermediate representation for garment synthesis. The hybrid person representation  $\mathbf{I}_{hybrid} \in \mathbb{R}^{6 \times H \times W}$  is a combination of virtual measurement garment  $\mathbf{I}_{vm}$  and human body semantic map  $\mathbf{I}_{sdp}$ , and can be formally represented as:

$$\mathbf{I}_{hybrid} = \mathbf{I}_{vm} \oplus \mathbf{I}_{sdp} \quad (2)$$

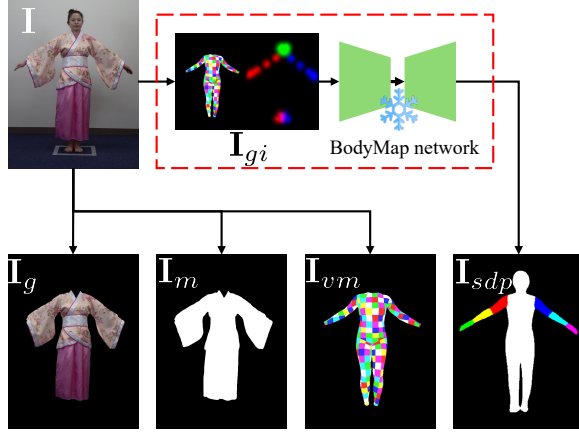


**Figure 7.** Per-garment dataset generation from recorded video frames of the human model. Unlike [54] that directly obtain the human body semantic map using DensePose [17], we extract garment-invariant representation and then transform it into the semantic map by our trained BodyMap network (red dashed box).

where  $I_{vm}$  captures the 3D pose of the human body which is crucial for 360° virtual try-on,  $I_{sdp}$  provides pixel-level alignment guidance in 2D image space.

Unlike [54], which trains the garment synthesis network on a per-frame basis, we train a Recurrent Garment Synthesis (ReGarSyn) network with sequential data to enhance the temporal consistency of the try-on results. We insert a lightweight ConvLSTM [46] module into pix2pixHD [53] to obtain our ReGarSyn network.

As illustrated in Figure 13, given an input sequence  $\{I_{hybrid}^1, I_{hybrid}^2, \dots, I_{hybrid}^N\}$  and a corresponding ground truth output sequence  $\{(I_g^1, I_m^1), (I_g^2, I_m^2), \dots, (I_g^N, I_m^N)\}$ , the input and output of the ReGarSyn network at time step  $t$  can be represented as:

$$\tilde{I}_g^t, \tilde{I}_m^t, C^t, \mathcal{H}^t = \text{ReGarSyn}(I_{hybrid}^t, C^{t-1}, \mathcal{H}^{t-1}) \quad (3)$$

Here,  $\tilde{I}_g^t$  and  $\tilde{I}_m^t$  denote the synthesized garment image and mask at time step  $t$ , respectively.  $C$  and  $\mathcal{H}$  represent the cell state and hidden state of the ConvLSTM module, capturing temporal dependencies across the sequence.

The loss function  $\mathcal{L}$  can be defined as:

$$\mathcal{L} = \sum_{t=1}^N \text{PerFrame}(\tilde{I}_g^t \oplus \tilde{I}_m^t, I_g^t \oplus I_m^t) \quad (4)$$

where  $\text{PerFrame}(\cdot, \cdot)$  denotes the per-frame loss function from pix2pixHD [53]. Explicit temporal consistency loss functions are not employed, as the supervision provided by temporally consistent ground truth data inherently ensures temporal coherence.

### 3.6 Inference Pipeline of Virtual Try-On

During inference, we assume the user is wearing a tight-fitting garment, which allows us to efficiently extract a semantic map of the human body using DensePose [17]. This assumption is practical and user-friendly, as it avoids the need for specialized wearable devices required by a prior approach [8].

As illustrated in Figure 10, given an input frame  $I^t$  at time step  $t$ , we extract the virtual measurement garment  $I_{vm}^t$  using BEV [48], and obtain the human body semantic map  $I_{sdp}^t$  via DensePose [17]. Both processes are computationally efficient and suitable for real-time applications. Subsequently, as described in Equation 3, we input them together with  $C^{t-1}$  and  $\mathcal{H}^{t-1}$  from the previous time step to the trained ReGarSyn network to obtain the synthesized garment image  $\tilde{I}_g^t$  and mask  $\tilde{I}_m^t$ . Finally, we composite them onto the input frame to obtain the try-on result  $I_o^t$ :

$$I_o^t = I^t \odot (1 - \tilde{I}_m^t) + \tilde{I}_g^t \odot \tilde{I}_m^t \quad (5)$$

where  $\odot$  denotes element-wise multiplication.

Our recurrent framework facilitates temporally coherent virtual try-on outputs over arbitrarily long input sequences while maintaining real-time performance and a constant memory footprint.

## 4 Experiments

### 4.1 Experiment Setting

**Per-garment datasets.** We collected per-garment datasets for four loose-fitting garments, including a hanfu, a down jacket, a hanbok, and a dress, using the same human model. Each dataset contains approximately 3,000 images. Additionally, we recorded a video of the same human model wearing a tight-fitting garment and performing similar movements for evaluation purposes.

**Implementation details.** We set the resolution of the BodyMap network to  $512 \times 384$  and the ReGarSyn networks to  $576 \times 432$ . For each garment, we trained a per-garment model using the corresponding per-garment dataset. We trained each model on an NVIDIA RTX 4090 GPU for 40 epochs, with a learning rate of  $2 \times 10^{-4}$ . During training, we randomly sampled clips ranging in length from 8 to 60 frames. We use the Adam optimizer with  $\beta_1 = 0.5$  and  $\beta_2 = 0.999$ . The training duration for a garment-specific model was approximately 12 hours.

**Comparison setting.** We conduct both qualitative and quantitative evaluations of our method, using the prior per-garment virtual try-on approach [54] as the baseline for comparison. Additionally, we compare our results with OOTDiffusion [57] and ViViD [12], which represent state-of-the-art image-based and video-based virtual try-on methods, respectively. Due to mismatches in input and output formats, retraining OOTDiffusion and ViViD on our datasets is not

feasible, limiting the fairness of direct comparisons. Nonetheless, we include these methods to demonstrate that their reliance on a universal network for generalization across all garment types proves inadequate in practice, especially for rarely seen garments.

#### 4.2 Qualitative Evaluation

We present a qualitative comparison of image quality among OOTDiffusion [57], ViViD [12], the baseline method [54], and our method in Figure 8. Both OOTDiffusion and ViViD produce poor results for these loose-fitting garments, which supports our assertion that training a universal network on frequently seen garments cannot generalize well to all types of garments.

In the results produced by the baseline method, noticeable flaws appear in regions with loose-fitting garments—such as the wide sleeves of the hanfu (first row), the skirt hems of the hanbok (third row), and the hems of the dress (fourth row). These artifacts support our assertion that the baseline method struggles with discrepancies in input data distribution between the training and inference stages due to occlusions introduced by loose-fitting garments. While the down jacket (second row) does not exhibit such artifacts due to its relatively tight-fitting structure, it reveals temporal inconsistencies attributable to the baseline’s frame-by-frame garment synthesis strategy, as further evidenced by the quantitative results in Section 4.3. For a more intuitive video comparison, please refer to the supplementary video.



**Figure 8.** Qualitative comparison of our method against OOTDiffusion [57], ViViD [12], and the baseline method [54].

Furthermore, to demonstrate the generalization ability of our ReGarSyn networks trained on per-garment datasets

collected by a single human model, we present the virtual try-on results for unseen body shapes in ???. This figure indicates that our strategy of using only one human model for each per-garment dataset is sufficient, as the ReGarSyn network successfully generalizes to a wide range of body shapes.

#### 4.3 Quantitative Evaluation

Since collecting paired ground truth data for loose-fitting garment virtual try-on is impractical, we adopt evaluation metrics that do not rely on such data. Specifically, we use Kernel Inception Distance (KID) and Fréchet Inception Distance (FID) to assess image quality. To evaluate both image quality and temporal consistency, we employ Video Fréchet Inception Distance (VFID), which leverages the I3D backbone [2]. These metrics are computed using two videos: one showcasing the generated virtual try-on result and the other depicting the same person wearing the actual loose-fitting garment. Although the videos exhibit similar human motion, they are not strictly synchronized.

We report the quantitative results for four loose-fitting garments individually in Table 1. As shown in the table, both OOTDiffusion [57] and ViViD [12] perform significantly worse than the baseline and our proposed method, which is consistent with the qualitative observations discussed in Section 4.2. Although the baseline occasionally surpasses our method in certain image quality metrics, our approach achieves comparable scores overall and consistently outperforms all others in VFID across all garments. This highlights the strength of our method in maintaining both temporal consistency and visual fidelity.

#### 4.4 Frame Rate Comparison

We compare the frame rate of our method against OOTDiffusion [57], ViViD [12], the baseline approach [54], and a variant of our model that shares the same architecture but excludes the ConvLSTM module and is trained on a per-frame basis ("ours w/o ConvLSTM"). This variant is included to evaluate the impact of the ConvLSTM module on frame rate performance. All frame rates are measured using an NVIDIA RTX 4090 GPU.

As shown in Table 2, both OOTDiffusion and ViViD exhibit frame rates that fall short of real-time requirements. The baseline achieves the highest frame rate, while the "ours w/o ConvLSTM" variant, which incorporates additional processing for the DensePose map, performs slightly slower. Our proposed method integrates a ConvLSTM module, resulting in a 14% reduction in frame rate. Despite this, it maintains a frame rate of 10.5 frames per second, which remains adequate for real-time use.

**Table 1.** Quantitative comparison with other approaches and ablation study on the ConvLSTM module.

Method	Hanfu			Down jacket			Hanbok			Dress		
	KID↓	FID↓	VFID↓	KID↓	FID↓	VFID↓	KID↓	FID↓	VFID↓	KID↓	FID↓	VFID↓
OOTDiffusion [57]	0.073	77.27	1.138	0.180	154.43	1.234	0.257	187.30	1.359	0.116	100.47	1.036
ViViD [12]	0.190	153.88	1.266	0.200	173.29	1.115	0.439	285.40	1.254	0.125	105.57	0.996
Baseline [54]	0.043	51.25	1.041	0.102	97.81	1.027	0.022	28.85	0.942	<b>0.071</b>	<b>66.75</b>	0.992
Ours w/o ConvLSTM	0.037	44.24	1.027	0.102	98.41	1.029	<b>0.020</b>	<b>26.92</b>	0.933	0.072	67.00	0.981
Ours	<b>0.034</b>	<b>42.88</b>	<b>1.025</b>	<b>0.099</b>	<b>96.86</b>	<b>1.024</b>	0.021	27.01	<b>0.930</b>	0.073	67.26	<b>0.980</b>

**Table 2.** Comparison of frame rates. The introduction of the ConvLSTM module results in a slight decrease in frame rate but remains sufficient for real-time performance use.

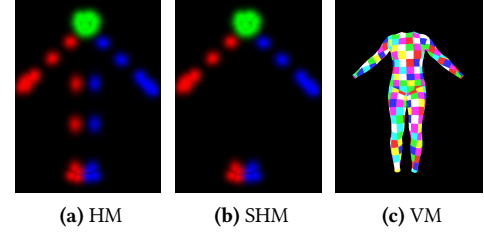
Method	Frame rate (fps) ↑
OOTDiffusion [57]	0.32
ViViD [12]	1.32
Baseline [54]	<b>12.38</b>
Ours w/o ConvLSTM	12.15
Ours	10.50

#### 4.5 Ablation Study on Garment-Invariant Representation

To demonstrate the necessity of our proposed garment-invariant representation and its components, we conduct ablation studies with the following alternative approaches for human body semantic map estimation:

- **DP:** Directly using DensePose [17] to obtain the human body semantic map without any intermediate representation. This is to demonstrate the benefit of our proposed garment-invariant representation.
- **HM:** Using heatmaps without removing any joints as the intermediate representation (Figure 9(a)). This is to show the significance of removing garment-sensitive joints.
- **SHM:** Using heatmaps without garment-sensitive joints as the intermediate representation (Figure 9(b)). This reveals the importance of the virtual measurement garment [55].
- **VM:** Using virtual measurement garment [55] as the intermediate representation (Figure 9(c)). This demonstrates the importance of joint heatmaps.

We lack ground truth data for estimating human body semantic maps under loose-fitting garments, as obtaining paired images of the same person in identical poses wearing both tight-fitting and loose-fitting clothing is not feasible. Therefore, we can only conduct a qualitative comparison. The metrics used in Section 4.3 are unsuitable here since they cannot accurately reflect how well the semantic maps align with the human body.

**Figure 9.** Three alternative intermediate representations used in ablation study for human body semantic map estimation.

As shown in Figure 15, our proposed garment-invariant representation enables reliable human body semantic map estimation. The semantic maps estimated by DensePose suffer from occlusion, e.g., the lower body region is missing due to the occlusion of the hanbok skirt (first row, DP column). Using joint heatmaps that include garment-sensitive joints results in inflated semantic maps (HM column). Utilizing joint heatmaps without garment-sensitive joints fails to provide sufficient information for semantic map estimation, resulting in distorted and incomplete results (SHM column). Relying solely on the virtual measurement garments does not provide pixel-level guidance for semantic map estimation, resulting in limbs being placed in incorrect regions (second row, VM column).

#### 4.6 Ablation Study on ConvLSTM Module

We evaluate the effectiveness of the ConvLSTM module in enhancing temporal consistency through both qualitative and quantitative comparisons with a variant without ConvLSTM ("ours w/o ConvLSTM"), as described in Section 4.4.

To better illustrate the presence of jittering artifacts, we visualize the absolute differences between consecutive output frames using heatmaps, as shown in Figure 16. These visualizations reveal that the "ours w/o ConvLSTM" variant exhibits noticeable jittering artifacts, particularly along the boundary of the loose skirt, which tends to vary in appearance even when the human remains relatively static. In contrast, our method, which incorporates the ConvLSTM module, achieves notably improved temporal consistency



across frames. For a more intuitive comparison, please refer to the supplementary video.

## 5 Limitations and Future Work

In addition to the common limitations mentioned by [54], such as the necessity of data capture for each garment, the original garment is not removed, and inaccurate composition masks, we would like to highlight two limitations and their future work as follows:

**Inability to convey actual size and fit.** While our method generates visually plausible virtual try-on results for a wide range of body shapes and provides useful styling references (??), it does not validate the suitability of garment sizing due to the lack of actual user body measurements. This limitation is common among most existing image-based virtual try-on approaches. A promising future direction is to develop a garment synthesis framework that incorporates user-provided body dimensions to enable more accurate and personalized virtual try-on experiences.

**Limitation in modeling transient physical dynamics.** Although our recurrent framework incorporates temporal information by conditioning garment synthesis on preceding frames, its primary objective is to enforce inter-frame consistency rather than to model the transient physical dynamics of loose-fitting garments. The datasets we collected using the method of [54] comprise sequences of humans rotating in place, offering inadequate motion diversity for capturing the complex physical behaviors of loose garments. To address this limitation, a novel dataset collection method that introduces a broader range of motion while remaining accessible needs to be explored.

## 6 Conclusion

We introduce a novel per-garment approach that is the first to enable real-time and temporally coherent virtual try-on for loose-fitting garments. To enhance the quality of synthesized images, we propose a garment-invariant representation that facilitates accurate estimation of human body semantic maps under loose-fitting garments during per-garment dataset generation. This representation effectively mitigates the distribution gap between the training and inference stages of our garment synthesis network, resulting in significantly improved visual fidelity. To ensure temporal consistency, we propose a recurrent framework that leverages temporal dependencies for garment synthesis. Our inference pipeline demonstrates sufficient efficiency to support real-time virtual try-on and can process input frames of arbitrary length. Through extensive qualitative and quantitative evaluations, we demonstrate that our method outperforms existing approaches in both image quality and temporal consistency. We also conduct ablation studies to validate the effectiveness of the garment-invariant representation and the recurrent synthesis framework.

## References

- [1] Yukang Cao, Masoud Hadi, Liang Pan, and Ziwei Liu. 2024. GS-VTON: Controllable 3D Virtual Try-on with Gaussian Splatting. *arXiv preprint arXiv:2410.05259* (2024).
- [2] Joao Carreira and Andrew Zisserman. 2017. Quo vadis, action recognition? a new model and the kinetics dataset. In *proceedings of the IEEE Conference on Computer Vision and Pattern Recognition*. 6299–6308.
- [3] Andrés Casado-Elvira, Marc Comino Trinidad, and Dan Casas. 2022. Pergamo: Personalized 3d garments from monocular video. In *Computer Graphics Forum*, Vol. 41. Wiley Online Library, 293–304.
- [4] Chieh-Yun Chen, Ling Lo, Pin-Jui Huang, Hong-Han Shuai, and Wen-Huang Cheng. 2021. Fashionmirror: Co-attention feature-remapping virtual try-on with sequential template poses. In *Proceedings of the IEEE/CVF International Conference on Computer Vision*. 13809–13818.
- [5] Haodong Chen, Yongle Huang, Haojian Huang, Xiangsheng Ge, and Dian Shao. 2024. Gaussianvton: 3d human virtual try-on via multi-stage gaussian splatting editing with image prompting. *arXiv preprint arXiv:2405.07472* (2024).
- [6] Yiwen Chen, Zilong Chen, Chi Zhang, Feng Wang, Xiaofeng Yang, Yikai Wang, Zhongang Cai, Lei Yang, Huaping Liu, and Guosheng Lin. 2024. Gaussianeditor: Swift and controllable 3d editing with gaussian splatting. In *Proceedings of the IEEE/CVF conference on computer vision and pattern recognition*. 21476–21485.
- [7] Seunghwan Choi, Sunghyun Park, Minsoo Lee, and Jaegul Choo. 2021. Viton-hd: High-resolution virtual try-on via misalignment-aware normalization. In *Proceedings of the IEEE/CVF conference on computer vision and pattern recognition*. 14131–14140.
- [8] Toby Chong, I-Chao Shen, Nobuyuki Umetani, and Takeo Igarashi. 2021. Per garment capture and synthesis for real-time virtual try-on. In *The 34th Annual ACM Symposium on User Interface Software and Technology*. 457–469.
- [9] Gabriel Cirio, Jorge Lopez-Moreno, David Miraut, and Miguel A Otaduy. 2014. Yarn-level simulation of woven cloth. *ACM Transactions on Graphics (TOG)* 33, 6 (2014), 1–11.
- [10] Haoye Dong, Xiaodan Liang, Xiaohui Shen, Bowen Wu, Bing-Cheng Chen, and Jian Yin. 2019. Fw-gan: Flow-navigated warping gan for video virtual try-on. In *Proceedings of the IEEE/CVF international conference on computer vision*. 1161–1170.
- [11] Jiahua Dong and Yu-Xiong Wang. 2023. Vica-nerf: View-consistency-aware 3d editing of neural radiance fields. *Advances in Neural Information Processing Systems* 36 (2023), 61466–61477.
- [12] Zixun Fang, Wei Zhai, Aimin Su, Hongliang Song, Kai Zhu, Mao Wang, Yu Chen, Zhiheng Liu, Yang Cao, and Zheng-Jun Zha. 2024. ViViD: Video Virtual Try-on using Diffusion Models. *arXiv preprint arXiv:2405.11794* (2024).
- [13] Abolfazl Farahani, Sahar Voghoei, Khaled Rasheed, and Hamid R Arabnia. 2021. A brief review of domain adaptation. *Advances in data science and information engineering: proceedings from ICDATA 2020 and IKE 2020* (2021), 877–894.
- [14] Yao Feng, Jinlong Yang, Marc Pollefeys, Michael J Black, and Timo Bolkart. 2022. Capturing and animation of body and clothing from monocular video. In *SIGGRAPH Asia 2022 Conference Papers*. 1–9.
- [15] Artur Grigorev, Michael J Black, and Otmar Hilliges. 2023. Hood: Hierarchical graphs for generalized modelling of clothing dynamics. In *Proceedings of the IEEE/CVF Conference on Computer Vision and Pattern Recognition*. 16965–16974.
- [16] Peng Guan, Loretta Reiss, David A Hirshberg, Alexander Weiss, and Michael J Black. 2012. Drape: Dressing any person. *ACM Transactions on Graphics (ToG)* 31, 4 (2012), 1–10.
- [17] Rıza Alp Güler, Natalia Neverova, and Iasonas Kokkinos. 2018. Densepose: Dense human pose estimation in the wild. In *Proceedings of the IEEE conference on computer vision and pattern recognition*. 7297–7306.
- [18] Oshri Halimi, Egor Larionov, Zohar Barzelay, Philipp Herholz, and Tuur Stuyck. 2023. Physgraph: Physics-based integration using graph

- neural networks. *arXiv preprint arXiv:2301.11841* (2023).
- [19] Zijian He, Yuwei Ning, Yipeng Qin, Wangrun Wang, Sibe Yang, Liang Lin, and Guanbin Li. 2025. VTON 360: High-fidelity virtual try-on from any viewing direction. *arXiv preprint arXiv:2503.12165* (2025).
  - [20] Judy Hoffman, Dequan Wang, Fisher Yu, and Trevor Darrell. 2016. Fcns in the wild: Pixel-level adversarial and constraint-based adaptation. *arXiv preprint arXiv:1612.02649* (2016).
  - [21] Phillip Isola, Jun-Yan Zhu, Tinghui Zhou, and Alexei A Efros. 2017. Image-to-image translation with conditional adversarial networks. In *Proceedings of the IEEE conference on computer vision and pattern recognition*. 1125–1134.
  - [22] Nikolay Jetchev and Urs Bergmann. 2017. The conditional analogy gan: Swapping fashion articles on people images. In *Proceedings of the IEEE international conference on computer vision workshops*. 2287–2292.
  - [23] Jianbin Jiang, Tan Wang, He Yan, and Junhui Liu. 2022. Clothformer: Taming video virtual try-on in all module. In *Proceedings of the IEEE/CVF Conference on Computer Vision and Pattern Recognition*. 10799–10808.
  - [24] Jonathan M Kaldor, Doug L James, and Steve Marschner. 2008. Simulating knitted cloth at the yarn level. In *ACM SIGGRAPH 2008 papers*. 1–9.
  - [25] Johanna Karras, Yingwei Li, Nan Liu, Luyang Zhu, Innfarn Yoo, Andreas Lugmayr, Chris Lee, and Ira Kemelmacher-Shlizerman. 2024. Fashion-VDM: Video Diffusion Model for Virtual Try-On. *arXiv preprint arXiv:2411.00225* (2024).
  - [26] Bernhard Kerbl, Georgios Kopanas, Thomas Leimkühler, and George Drettakis. 2023. 3d gaussian splatting for real-time radiance field rendering. *ACM Trans. Graph.* 42, 4 (2023), 139–1.
  - [27] Rawal Khrodar, Timur Bagautdinov, Julieta Martinez, Su Zhaoen, Austin James, Peter Selednik, Stuart Anderson, and Shunsuke Saito. 2024. Sapiens: Foundation for human vision models. In *European Conference on Computer Vision*. Springer, 206–228.
  - [28] Jeongho Kim, Guojung Gu, Minhho Park, Sunghyun Park, and Jaegul Choo. 2024. Stableviton: Learning semantic correspondence with latent diffusion model for virtual try-on. In *Proceedings of the IEEE/CVF Conference on Computer Vision and Pattern Recognition*. 8176–8185.
  - [29] Zorah Lahner, Daniel Cremers, and Tony Tung. 2018. Deepwrinkles: Accurate and realistic clothing modeling. In *Proceedings of the European conference on computer vision (ECCV)*. 667–684.
  - [30] Sangyun Lee, Gyojung Gu, Sunghyun Park, Seunghwan Choi, and Jaegul Choo. 2022. High-resolution virtual try-on with misalignment and occlusion-handled conditions. In *European Conference on Computer Vision*. Springer, 204–219.
  - [31] Zhe Li, Zerong Zheng, Lizhen Wang, and Yebin Liu. 2024. Animatable Gaussians: Learning Pose-dependent Gaussian Maps for High-fidelity Human Avatar Modeling. In *Proceedings of the IEEE/CVF Conference on Computer Vision and Pattern Recognition (CVPR)*. 19711–19722.
  - [32] Siyou Lin, Zhe Li, Zhaoqi Su, Zerong Zheng, Hongwen Zhang, and Yebin Liu. 2024. Layga: Layered gaussian avatars for animatable clothing transfer. In *ACM SIGGRAPH 2024 Conference Papers*. 1–11.
  - [33] Matthew Loper, Naureen Mahmood, Javier Romero, Gerard Pons-Moll, and Michael J Black. 2015. SMPL: A Skinned Multi-Person Linear Model. *Acm Transactions on Graphics* 34, Article 248 (2015).
  - [34] Ben Mildenhall, Pratul P Srinivasan, Matthew Tancik, Jonathan T Barron, Ravi Ramamoorthi, and Ren Ng. 2021. Nerf: Representing scenes as neural radiance fields for view synthesis. *Commun. ACM* 65, 1 (2021), 99–106.
  - [35] Rahul Narain, Armin Samii, and James F O'brien. 2012. Adaptive anisotropic remeshing for cloth simulation. *ACM transactions on graphics (TOG)* 31, 6 (2012), 1–10.
  - [36] Xiaoyu Pan, Jiaming Mai, Xinwei Jiang, Dongxue Tang, Jingxiang Li, Tianjia Shao, Kun Zhou, Xiaogang Jin, and Dinesh Manocha. 2022. Predicting loose-fitting garment deformations using bone-driven motion networks. In *ACM SIGGRAPH 2022 Conference Proceedings*. 1–10.
  - [37] Chaitanya Patel, Zhouyingcheng Liao, and Gerard Pons-Moll. 2020. Tailornet: Predicting clothing in 3d as a function of human pose, shape and garment style. In *Proceedings of the IEEE/CVF conference on computer vision and pattern recognition*. 7365–7375.
  - [38] Nikhila Ravi, Valentin Gabeur, Yuan-Ting Hu, Ronghang Hu, Chaitanya Ryali, Tengyu Ma, Haitham Khedr, Roman Rädle, Chloe Rolland, Laura Gustafson, et al. 2024. Sam 2: Segment anything in images and videos. *arXiv preprint arXiv:2408.00714* (2024).
  - [39] Amélie Royer, Konstantinos Bousmalis, Stephan Gouws, Fred Bertsch, Inbar Mosseri, Forrester Cole, and Kevin Murphy. 2020. Xgan: Unsupervised image-to-image translation for many-to-many mappings. In *Domain Adaptation for Visual Understanding*. Springer, 33–49.
  - [40] Swami Sankaranarayanan, Yogesh Balaji, Carlos D Castillo, and Rama Chellappa. 2018. Generate to adapt: Aligning domains using generative adversarial networks. In *Proceedings of the IEEE conference on computer vision and pattern recognition*. 8503–8512.
  - [41] Igor Santesteban, Miguel A Otaduy, and Dan Casas. 2019. Learning-based animation of clothing for virtual try-on. In *Computer Graphics Forum*, Vol. 38. Wiley Online Library, 355–366.
  - [42] Igor Santesteban, Miguel A Otaduy, and Dan Casas. 2022. Snug: Self-supervised neural dynamic garments. In *Proceedings of the IEEE/CVF Conference on Computer Vision and Pattern Recognition*. 8140–8150.
  - [43] Igor Santesteban, Nils Thuerey, Miguel A Otaduy, and Dan Casas. 2021. Self-supervised collision handling via generative 3d garment models for virtual try-on. In *Proceedings of the IEEE/CVF Conference on Computer Vision and Pattern Recognition*. 11763–11773.
  - [44] Masahiro Sekine, Kaoru Sugita, Frank Perbet, Björn Stenger, and Masashi Nishiyama. 2014. Virtual fitting by single-shot body shape estimation. In *Int. Conf. on 3D Body Scanning Technologies*, Vol. 406. Citeseer, 413.
  - [45] Andrew Selle, Jonathan Su, Geoffrey Irving, and Ronald Fedkiw. 2008. Robust high-resolution cloth using parallelism, history-based collisions, and accurate friction. *IEEE transactions on visualization and computer graphics* 15, 2 (2008), 339–350.
  - [46] Xingjian Shi, Zhouong Chen, Hao Wang, Dit-Yan Yeung, Wai-Kin Wong, and Wang-chun Woo. 2015. Convolutional LSTM network: A machine learning approach for precipitation nowcasting. *Advances in neural information processing systems* 28 (2015).
  - [47] Dan Song, Xuanpu Zhang, Juan Zhou, Weizhi Nie, Ruofeng Tong, and An-An Liu. 2023. Image-Based Virtual Try-On: A Survey. *arXiv preprint arXiv:2311.04811* (2023).
  - [48] Yu Sun, Wu Liu, Qian Bao, Yili Fu, Tao Mei, and Michael J Black. 2022. Putting people in their place: Monocular regression of 3d people in depth. In *Proceedings of the IEEE/CVF Conference on Computer Vision and Pattern Recognition*. 13243–13252.
  - [49] Eric Tzeng, Judy Hoffman, Trevor Darrell, and Kate Saenko. 2015. Simultaneous deep transfer across domains and tasks. In *Proceedings of the IEEE international conference on computer vision*. 4068–4076.
  - [50] Eric Tzeng, Judy Hoffman, Kate Saenko, and Trevor Darrell. 2017. Adversarial discriminative domain adaptation. In *Proceedings of the IEEE conference on computer vision and pattern recognition*. 7167–7176.
  - [51] Eric Tzeng, Judy Hoffman, Ning Zhang, Kate Saenko, and Trevor Darrell. 2019. Deep domain confusion: Maximizing for domain invariance. *arXiv* 2014. *arXiv preprint arXiv:1412.3474* (2019).
  - [52] Haoyu Wang, Zhilu Zhang, Donglin Di, Shiliang Zhang, and Wangmeng Zuo. 2024. MV-VTON: Multi-View Virtual Try-On with Diffusion Models. *arXiv preprint arXiv:2404.17364* (2024).
  - [53] Ting-Chun Wang, Ming-Yu Liu, Jun-Yan Zhu, Andrew Tao, Jan Kautz, and Bryan Catanzaro. 2018. High-resolution image synthesis and semantic manipulation with conditional gans. In *Proceedings of the IEEE conference on computer vision and pattern recognition*. 8798–8807.
  - [54] Zaiqiang Wu, Yechen Li, Jingyuan Liu, Yuki Shibata, Takayuki Hori, I-Chao Shen, and Takeo Igarashi. 2025. Low-Barrier Dataset Collection with Real Human Body for Interactive Per-Garment Virtual Try-On.

- arXiv:2506.10468 [cs.GR]
- [55] Zaiqiang Wu, Jingyuan Liu, Long Hin Toby Chong, I-Chao Shen, and Takeo Igarashi. 2024. Virtual Measurement Garment for Per-Garment Virtual Try-On. In *Graphics Interface 2024*.
  - [56] Donglai Xiang, Fabian Prada, Timur Bagautdinov, Weipeng Xu, Yuan Dong, He Wen, Jessica Hodgins, and Chenglei Wu. 2021. Modeling clothing as a separate layer for an animatable human avatar. *ACM Transactions on Graphics (TOG)* 40, 6 (2021), 1–15.
  - [57] Yuhao Xu, Tao Gu, Weifeng Chen, and Chengcai Chen. 2024. Ootdif-fusion: Outfitting fusion based latent diffusion for controllable virtual try-on. *arXiv preprint arXiv:2403.01779* (2024).
  - [58] Zhengze Xu, Mengting Chen, Zhao Wang, Linyu Xing, Zhonghua Zhai, Nong Sang, Jinsong Lan, Shuai Xiao, and Changxin Gao. 2024. Tunnel Try-on: Excavating Spatial-temporal Tunnels for High-quality Virtual Try-on in Videos. *arXiv preprint arXiv:2404.17571* (2024).
  - [59] Jun-Yan Zhu, Taesung Park, Phillip Isola, and Alexei A Efros. 2017. Unpaired image-to-image translation using cycle-consistent adversarial networks. In *Proceedings of the IEEE international conference on computer vision*. 2223–2232.

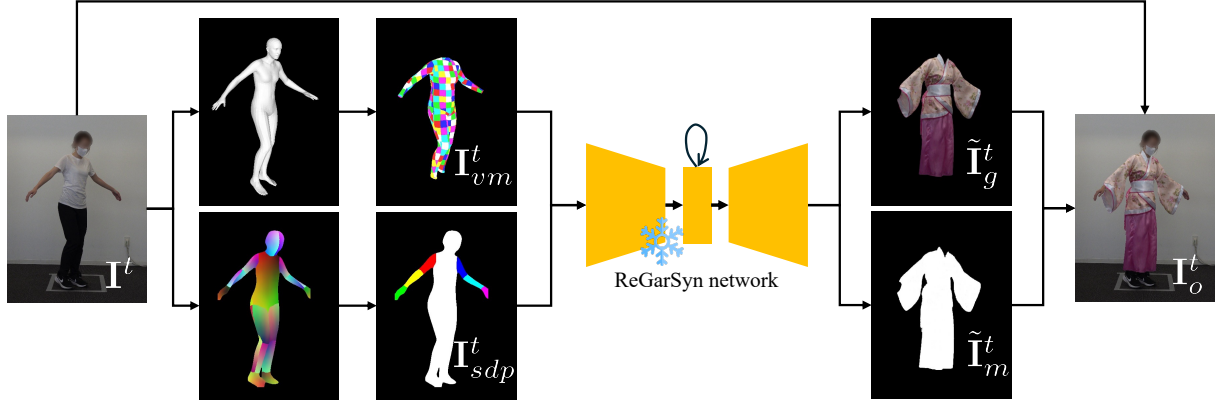
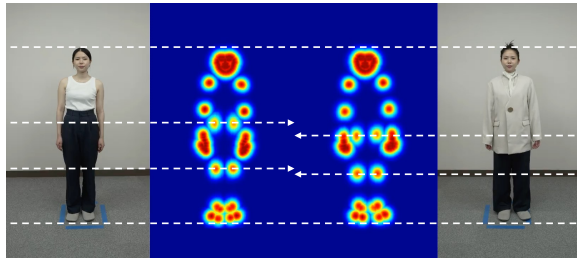
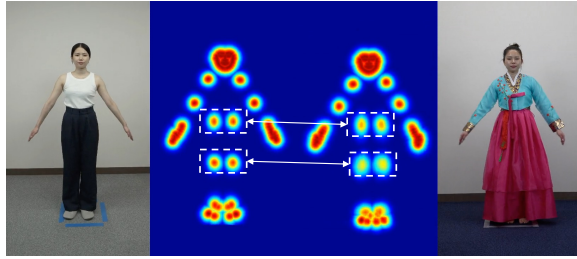


**Figure 10.** Detailed illustration of the inference pipeline for the ReGarSyn network.



(a) Garment's influence on the human joint locations.



(b) Garment's influence on human joint confidence scores.

**Figure 12.** Human joint estimation is not fully garment-invariant, especially for the knee and hip joints, whose positions and confidence scores are sensitive to garment variations.

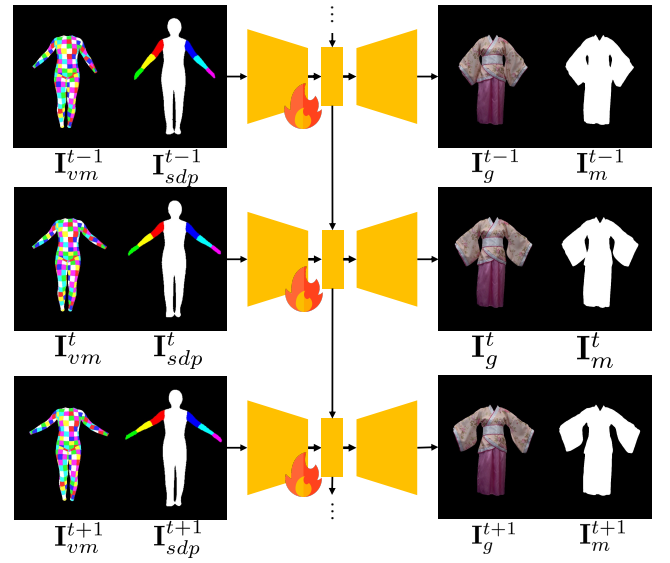


**Figure 13.** Detailed illustration of the ReGarSyn network training process.

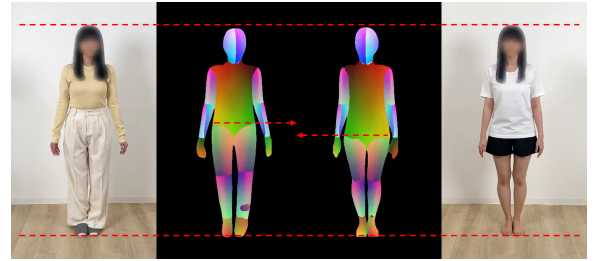


**Figure 11.** The boundary between the lower and upper body of the semantic map generated by DensePose [17] is sensitive to garment variation, even for tight-fitting garments.



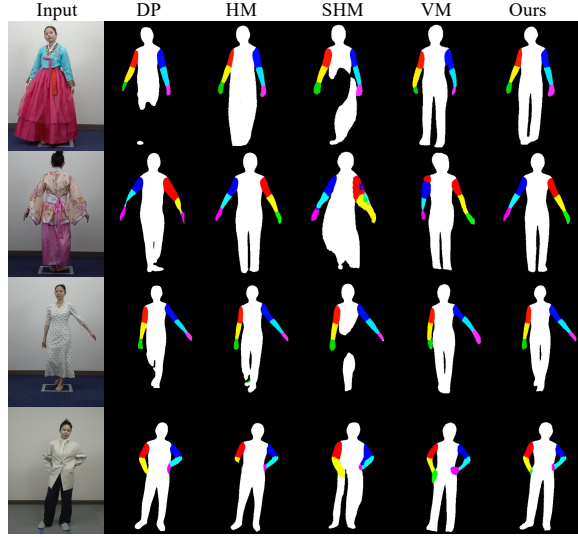


**Figure 15.** Ablation study on garment-invariant representation. **DP**: The semantic map estimated by DensePose [17] is not robust against loose-fitting garments. **HM**: Using joint heatmaps that include garment-sensitive joints leads to the inflation of the semantic map. **SHM**: Using joint heatmaps without garment-sensitive joints fails to provide adequate information for semantic map estimation. **VM**: Using solely virtual measurement garments fails to provide pixel-level accurate guidance for semantic maps.

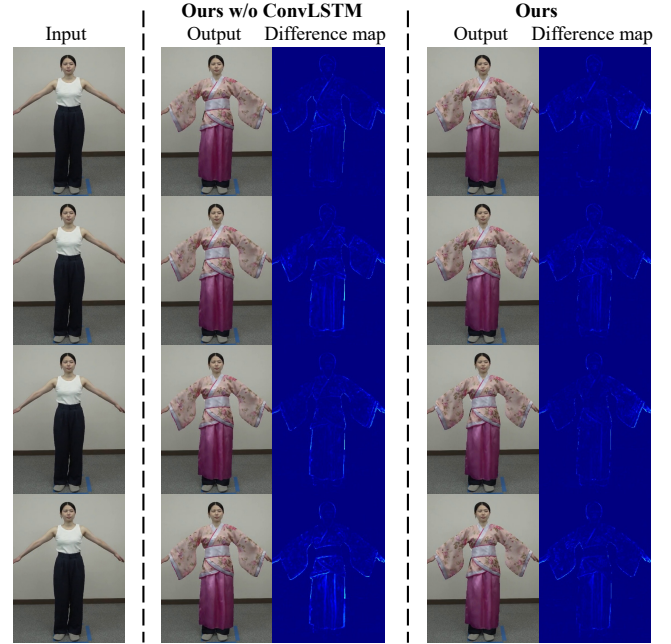


**Figure 16.** Ablation study on ConvLSTM module. The difference map visualizing absolute differences between consecutive output frames shows that the ConvLSTM module enhances temporal consistency effectively.